Equilibrium Shape of Si

D. J. Eaglesham, A. E. White, L. C. Feldman, N. Moriya, and D. C. Jacobson
AT&T Bell Laboratories, 600 Mountain Avenue, Murray Hill, New Jersey 07974
(Received 12 October 1992)

Small voids are formed in Si by MeV He implantation and annealing. We measure the equilibrium shape of these voids and hence extract the surface energy curve $\gamma(\theta)$ for Si. $\gamma(111)$ is the global minimum, with $\gamma(100) \approx 1.1\gamma(111)$ and all other cusps on the surface being relatively small. The experimental $\gamma(\theta)$ is compared with theoretical predictions and earlier experiments. Step energies obtained from $d\gamma/d\theta$ are $\approx 28 \pm 10$ meV/atom on (100) and $\approx 140 \pm 20$ meV/atom on (111); these values are compared with scanning tunneling microscopy experiments.

PACS numbers: 61.80.Jh, 61.16.Ch, 68.35.Bs

The equilibrium shape of a single crystal of Si remains unknown. Knowledge of this shape requires complete determination of the surface free energy function $\gamma(\theta)$. Experimental data provide several pieces of the puzzle: Thermal etching rates, faceting of miscut surfaces, and step energetics are all known for some surfaces. But the relative energies of the major facets have not yet been determined with precision. Ambiguities arise partly because surface science experiments are usually restricted to orientations close to a major crystal plane. Theoretical values are widely scattered and depend strongly on calculation techniques. Since the relative energetics of different surfaces play an important part in controlling rough growth morphologies, and since relative energies are a powerful test of our understanding of surface structure, the determination of the surface free energy function is increasingly significant. Here, we measure the equilibrium shape of voids formed by implantation of He into Si, and extract the surface free energy curve $\gamma(\theta)$.

The problem is an old one that has been addressed by many authors. Early experiments were hampered by questions regarding the role played by residual vacuum contaminants and defects in altering effects seen in thermal etching and annealing. Metals such as Pb proved amenable to experiments where deposited films were allowed to ball up and their shape was determined in detail [1]. For Si, oxidation and SiO desorption precluded similar studies, and interface energetics were determined by fracture [2], growth morphology [3,4], or implantation of noble gases [5]. This left a situation of some confusion and very little quantitative information. While fracture measurements access absolute surface energies (this is the only simple experimental technique for such measurements), only the (111) fracture surface can be measured [2]. The reconstruction is unknown, although the relevant surface energy is probably the cleaved (111) 2×1 surface [6]. Relative surface energies cannot be extracted from studies of growth morphology, but the observation of {311} growth facets on (111) growth surfaces [3] was used to suggest that {311} was a fairly low energy surface. Implantation of Ar, Kr, and Xe into Si [5] leaves gas-filled bubbles in a polycrystalline or heavily damaged matrix. The internal noble-gas pressure in the bubble (estimated as ≈ 1000 atm) plays an unknown role, but probably favors more spherical shapes. Moreover, bubble shapes observed in these systems were extremely nonuniform, so that while the authors concluded that {111}, {100}, and {311} were all low energy and {111} was probably lowest, there was no attempt at quantitative comparison and the relative surface energies could not be extracted from a Wulff construction.

Recently, interest in noble gas implantation has been renewed by a series of experiments on He in Si [7]. Two important differences from heavier gas implants are apparent. First, the degree of implantation damage can be reduced so that samples are never fully amorphized during implantation and annealed samples are never polycrystalline. Second, He diffusion in Si is sufficiently fast to allow all the He to diffuse out of the free surface during a subsequent anneal, leaving *voids* rather than He bubbles [7]. Thus if we can anneal He-implanted samples at a high enough temperature so that diffusion around the internal surfaces of the voids is sufficient, all voids should attain the equilibrium shape. The Wulff construction can then be used to extract the complete surface free energy plot of Si. There are two important approximations to be made in extracting the $\gamma(\theta)$ plot from the Wulff construction; first that the internal void shape is identical to the external crystal shape, and second that the void is sufficiently large for corner energy terms to be negligible compared to surface energy terms. These two approximations turn out to be equivalent (in the large-void limit the void shape is identical to crystal shape). The void sizes studied here lie at the limit of validity of these approximations. For a void diameter ≈ 100 Å, atoms at corner intersections represent $\approx 1\%$ of the total number of surface atoms. This will mean that the general void shape (large facets) will accurately reflect $\gamma(\theta)$, but the details of the shape near the corners must be interpreted with caution. (For details of this and other subtleties in relating shape to surface free energy the reader is referred to Herring's classic description [8].)

Si surface diffusion has been studied for individual adatoms down to room temperature with a relatively small (0.6 eV) activation energy [9]. However, to equilibrate a bulk shape such as a void we require adatom re-

moval from steps, a considerably more energetic process. Measurements of the annealing of surface roughness on a ≈ 100 Å length scale [10] show that a 100 Å object can be completely annealed (into a flat surface in the roughness experiment) in a 10 min anneal at 400 °C. The rate increases with a ≈ 3.5 eV activation energy, a value close to the vacancy formation energy in Si. This is consistent with scanning tunneling microscopy (STM) data on Ostwald ripening of step distributions produced by deposition [11]. 400–500 °C anneals for 10 min should thus easily allow full equilibration of voids with radii up to 500 Å. Complete removal of He from the initial bubbles turns out to be a more rigorous condition, requiring a 700 °C, 1 h anneal [7]. In addition to full equilibration and He removal, we also require negligible interactions with the Si surface (i.e., high energy He implantation) and minimum ion implantation damage and void-void interactions (low-dose, elevated-temperature implants). Since the He diffusion length is ≈ 1 mm for 700 °C, 1 h anneal, the implant energy, and hence the depth, should not have a significant effect on the He removal. The experiments described here were carried out using 1.2 MeV He implantation at 200–350 °C into Czochralski or float-zone (100) Si at doses of $\approx 10^{17}$ cm^{-2}, with the dose, temperature, and subsequent anneal being optimized for shape equilibration.

The criteria for assuring that one has equilibrium shapes are well established [1,8]: All shapes must be identical, shape should be size independent, and small objects should attain this shape first. In our study a series of anneals was carried out with the resulting microstructure being examined by transmission electron microscopy of (011) cross sections prepared by mechanical polishing and Ar-ion milling. As-implanted samples showed a thick region (≈ 4 μm) of undamaged Si above a 0.5 μm thick heavily damaged He-containing layer. Samples implanted at room temperature showed phase separation in this region into layers of amorphous Si containing He bubbles and bubble-free crystalline Si. Subsequent vacuum annealing (of bulk samples) in 10^{-8} Torr led to well-isolated voids at a density of $\approx 10^{17}$ cm^{-3} within a fully crystalline matrix containing a moderate density of stacking faults and dislocations ($\approx 10^{7}$ cm^{-2}); this voided layer was again separated from the surface by an undamaged layer 4 μm thick. This Si matrix appears to be of higher crystalline quality than comparable studies of low-energy high-concentration He implants [7], as expected. Shapes were examined using Fresnel contrast and high resolution. Fresnel images were recorded at a 400 symmetric three-beam diffraction condition as close as possible to the [011] zone axis (a weakly diffracting condition so that Fresnel contrast dominated, with all $\{hkk\}$ planes nearly vertical); through-focal series were used to determine the Fresnel fringe position in the small-defocus limit. High-resolution through-focal series allowed selection of optimum contrast with improved spatial resolution, but Fresnel fringe images of regions of thick cross section gave a far better statistical picture of any variations in void shape, and also allowed projection of the voids onto the high-tilt [010] and [111] directions.

Figure 1 shows a typical void shape for a sample annealed at 700 °C for 1 h in which void shape variations were minimized and could be associated with void pinning at defects (as opposed to any systematic size dependence). All voids showed the same broad features: large flat {111} facets, smaller curved {100} facets, and no detectable {110} or {311} facets (although these facets could be observed on some irregularly shaped voids, presumably at defects). The equilibrium shape of Si is thus (to a good approximation) a tetrakaidecahedron. Examination of images at [010] and [111] compared well with the expected projection of a tetrakaidecahedron (although since $\{hkk\}$ facets are dominating the shape, these images are less striking). The critical point to emphasize here is the apparent lack of sharp corners on these shapes. While we will discuss this in more detail later, a fully rounded shape is an essential criterion for the full γ plot to be represented in the equilibrium shape. This means that the Wulff construction can be reversed to find the surface energy at all orientations around the shape.

We now move to extracting quantitative data on the surface free energy from these void shapes via the Wulff construction [8]. The Wulff point ("center of mass") of a void is then defined as the intersection point of the perpendicular bisectors of two {111} facets: For the tetrakaidecahedron of Si voids this point also coincides with the intersection of the bisector of either {100} facet. Since there are no sharp facet intersections we can now measure the void radius r_i to each of the surface orientations i and then extract the relative γ_i for each orientation using the fact that $\gamma_i/r_i = \text{const}$ for a surface without

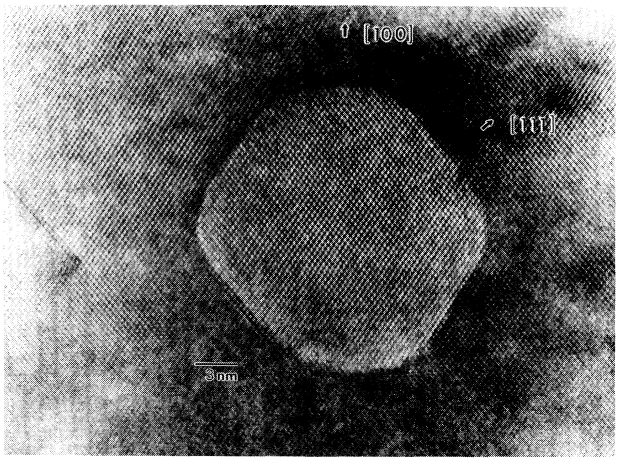

FIG. 1. The equilibrium shape of Si. Typical annealed void shape imaged in high resolution down ⟨110⟩ axis. Void is small enough to be completely enclosed in transmission electron microscopy cross section. Note flat {111} facets and rounded {100} facets, and curved facet intersections at {100} and near {311}.

sharp intersections. In practice, we measure radii with a 2° spacing, and average the data over several voids and several symmetry-equivalent orientations of the void. While all voids show similar shapes to the eye, very small changes in the shape make very significant modifications to the values extracted for surface free energy ratios.

An averaged and symmetrized $\gamma(\theta)$ plot is shown in Fig. 2, where we have normalized the relative energies to the {111}. The average is taken over three voids; the void-to-void variation in $\gamma(\theta)$ for a given orientation is $\pm 8\%$. This free energy plot obviously carries the same qualitative features evident from the shape alone: {111} is the most stable surface, {100} is the only other marked minimum in free energy, and the cusp at {111} is steeper (i.e., higher step energy). Now, however, we can quantify these qualitative statements. The most stable surface is {111} with the next lowest being {100}, a factor of 1.11 higher in energy. The {311} is slightly higher than {100} [$1.12\gamma(111)$] and does not have a detectable cusp, while {110} is the highest-energy {*hkk*} orientation [$1.16\gamma(111)$]. Repeating the averaging procedure for a different set of voids yields qualitatively similar results (minima at {100} and {111}, maxima at {110}, with {111} by far the dominant cusp), but suggests that quantitative values [such as the $\gamma(100)/\gamma(111)$ ratio] may vary (from ≈ 1.10 to ≈ 1.15).

These measurements thus represent the first determination of relative surface energies in Si, to $\pm 5\%$. The absolute scale on Fig. 2 can be set using Jaccodine's determination of $\gamma(111) = 1.23\ \mathrm{J\,m^{-2}}$ from fracture experiments [2]. While this strictly applies only to the 2×1 reconstruction formed on fracture surfaces [6], theoretical calculations suggest [12] that energy differences between the possible (111) reconstructions are fairly small ($\approx 10\%$), so this can be used to provide a quantitative estimate of all surface energies of Si. Hence we deduce the set of surface energies of Si shown in Table I. These values can be compared with theory (those papers where a single set of calculations has been performed for several orientations [13,14]). It seems clear that no current calculations provide a good match to the experimental data, and that the more sophisticated calculations are far from explaining even the most basic elements of the shape.

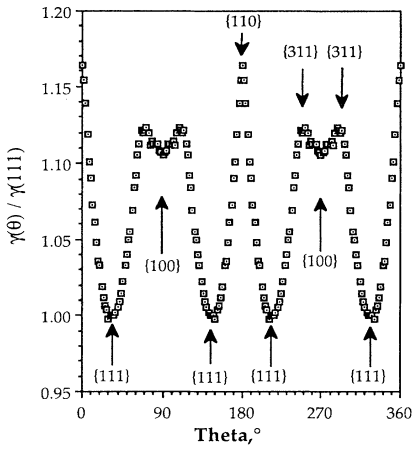

FIG. 2. The surface energy plot $\gamma(\theta)$ for Si. Surface energy ratios extracted by reverse Wulff construction from voids such as that in Fig. 1. Averaged over three particles and symmetrized on the assumption that {110} and {001} are both mirror planes.

In addition to surface energies, the quantitative data in Fig. 2 allow us to study $d\gamma/d\theta$ on the different surfaces, and thereby obtain information on steps. The discontinuity in $d\gamma/d\theta$ at the cusp on a surface is a measure of the step energy $\Delta(d\gamma/d\theta) = 2\beta/a$, where $\Delta(d\gamma/d\theta)$ is the discontinuity, β is the step energy, and a is the step height [15]. In the cusps on {111} and {100} we see discontinuities of $\Delta(d\gamma/d\theta) \approx 0.6\gamma(111)$/rad and $0.12\gamma(111)$/rad, respectively. Substituting Jaccodine's absolute value for $\gamma(111)$, and step heights of 3.13 and 1.36 Å, the measured faceting on the equilibrium shape suggests step energies of 5.7×10^{-11} and $1.0\times 10^{-11}\ \mathrm{J\,m^{-1}}$ for the {111} and {100} facets, respectively (for steps along [110], the significant step direction for both surfaces). These translate into atom energies (for each step atom) of 0.14 eV/atom (111) and 0.023 eV/atom (100). [Note that although Fig. 2 gives us $\gamma(\theta)/\gamma(111)$ to within $\pm 5\%$, step energies rely on $\Delta\gamma(\theta)$, which is determined only to within $\pm 30\%$.] For Si(100) we can compare with step energies previously determined from STM data (at approximately the same temperature) of 0.028 ± 0.002 eV/atom (low-energy "s_A" step) and 0.09 eV/atom (high-energy "s_B" step) [16]. The values obtained from our equilibrium shape determination thus appear to be close to that for the lower-energy step (as would be expected for an equilibrium step distribution), and provide confirmatory evidence for a step energy higher than that given by theoretical calculations (0.01 eV/atom [17]). For steps on (111) there appear to be no previous experimental measurements, although it may be estimated from thermally excited step distributions to be large (i.e., > 70 meV/atom) [18].

Finally, we discuss the qualitative form of the equilibrium shape. Given that only {111} and {100} facets are

TABLE I. Surface energies of the major {*hkk*} facets of Si from Fig. 2 [normalized with respect to (111) using Jaccodine's value [2]] with comparison to tight-binding calculations (Wilson, Todd, and Sutton [13]), and molecular dynamics with empirical potentials (Gilmer and Bakker [14], using Stillinger-Weber potential). Not all the calculations given here are for the experimentally observed reconstruction. We have estimated the {311} surface energy from [14] by interpolation.

Facet	Energy ($\mathrm{J\,m^{-2}}$)	Theory [13]	Theory [14]
(111)	1.23	1.41	1.405
(100)	1.36	1.34	1.488
(311)	1.38	1.378	≈ 1.48
(110)	1.43	1.573	1.721

large on the equilibrium shape, the question arises as to whether {311} and {110} orientations are present. The images appear to show rounded intersections at both {100}/{111} intersections (close to {311}) and {111}/{111} intersections ({110}). If these intersections are truly rounded then it follows [8] that although the energy of these surfaces is high relative to the other facets, both surfaces will be thermodynamically stable at these temperatures, and will not thermally etch onto the {111}/{100} combination. A secondary question is whether these orientations correspond to small cusps in the surface free energy function. Here we encounter problems associated with the small void diameter and consequently large proportion of facet-corner atoms. On atomic scales, derivative terms will force some rounding [8], and it is clear that these length scales are significant for the {110} and {311} surfaces. However, it is relatively easy now to invoke thermal etching data to demonstrate that {110} and {311} facets are stable. Since both {311} and {110} surfaces can be induced as facets in thermal annealing [19], we deduce that these orientations must have a small minimum in $\gamma(\theta)$. This means that a sufficiently large void would show small but measurable facets in these orientations in the shape (Fig. 1) and corresponding small minima in $\gamma(\theta)$ (Fig. 2). Since the rounding introduced by derivative terms is small spatially, this will introduce minima in Fig. 2 at {110} and {311}, but will not significantly affect the values determined for the energies of these surfaces given in Table I. For example, simple geometry shows that if $\gamma(311) < 1.13\gamma(111)$ then a (311) facet larger than the reconstructed unit cell for this surface would be visible in Fig. 1.

It is also worth noting that although {100} and {111} are by far the dominant minima in $\gamma(\theta)$, the appearance of {311} in Si growth morphology is widespread. We have reexamined Si growth on C-contaminated surfaces [19,20] because of questions regarding the vacuum in earlier growth experiments [3,4]; it is simple to confirm that growth of Si islands on (100) invariably leads to strong {311}/(100) faceting even in vacuum of $\approx 10^{-10}$ Torr. If there is indeed only a very small cusp in $\gamma(\theta)$ at {311}, the explanation for this must lie with the fact that a growth island has to make a transition from convex to concave shape at the island edge, Si being constrained to have a zero contact angle with Si. This then strongly favors the presence of facets that make small but finite angles with the surface, and means that the {311} facets in either (100) or (111) growth islands can be far more significant than those in the equilibrium shape. Similar conclusions apply to {110} facets, although very few authors have suggested that {110} is an unusually stable facet for Si. Our data on the equilibrium shape are thus perfectly consistent with all previous thermal etching experiments, with the exception that data on facets in annealing experiments imply small but finite cusps in $\gamma(\theta)$ at {110} and {311}.

In conclusion, we have measured the equilibrium shape of Si, and hence the complete surface free energy function $\gamma(\theta)$. The shape of annealed voids formed by He implantation is an approximate tetrakaidecahedron dominated by {100}/{111} facets. Existing theory does not agree with the experimentally determined Si surface energy ratios for different orientations. The results reported here are consistent with all previous thermal etching studies. Calculating $d\gamma/d\theta$ allows us to estimate step energies for important surfaces, and the values for (100) obtained in this way compare well with available STM data.

[1] J. C. Heyraud and J. J. Metois, Surf. Sci. **128**, 334 (1983).

[2] R. J. Jaccodine, J. Electrochem. Soc. **110**, 524 (1963); see also Comment by G. A. Wolff, J. Electrochem. Soc. **110**, 1293 (1963).

[3] G. R. Booker and B. A. Joyce, Philos. Mag. **14**, 301 (1966).

[4] B. A. Joyce, J. H. Neave, and B. E. Watts, Surf. Sci. **15**, 1 (1969).

[5] A. G. Cullis, T. E. Siedel, and R. L. Meek, J. Appl. Phys. **49**, 5188 (1978).

[6] R. M. Feenstra, J. A. Stroscio, and A. P. Fein, Surf. Sci. **181**, 295 (1987).

[7] C. C. Griffioen, J. H. Evans, P. C. de Jong, and A. van Veen, Nucl. Instrum. Methods Phys. Res., Sect. B **27**, 417 (1987); see also S. M. Myers, C. M. Foellstaedt, H. J. Stein, and W. R. Wampler, Phys. Rev. B **45**, 3914 (1992).

[8] C. Herring, in *Structure and Properties of Solid Surfaces,* edited by R. G. Gomer and C. S. Smith (University of Chicago Press, Chicago, 1953).

[9] Y.-W. Mo, J. Kleiner, M. B. Webb, and M. G. Lagally, Phys. Rev. Lett. **66**, 1998 (1991).

[10] Y. Y. Xie, G. H. Gilmer, E. A. Fitzgerald, and J. Michel, Mater. Res. Soc. Symp. Proc. **220**, 41 (1991).

[11] Y.-W. Mo, R. Kariotis, B. S. Swartzenruber, M. B. Webb, and M. G. Lagally, J. Vac. Sci. Technol. A **8**, 201 (1990).

[12] K. D. Brommer, M. Needels, B. E. Larson, and J. D. Joannopoulos, Phys. Rev. Lett. **68**, 1355 (1992); I. Stich, M. C. Payne, R. D. King-Smith, J.-S. Lin, and L. J. Clarke, Phys. Rev. Lett. **68**, 1351 (1992).

[13] J. H. Wilson, J. D. Todd, and A. P. Sutton, J. Phys. Condens. Matter **2**, 10259 (1990); **3**, 1971(E) (1991).

[14] G. H. Gilmer and A. F. Bakker, Mater. Res. Soc. Symp. Proc. **209**, 135 (1991).

[15] See, e.g., A. Zangwill, *Physics at Surfaces* (Cambridge Univ. Press, New York, 1988), p. 13.

[16] B. S. Schwatzenruber, Y.-W. Mo, R. Kariotis, M. G. Lagally, and M. B. Webb, Phys. Rev. Lett. **65**, 1913 (1990).

[17] J. D. Chadi, Phys. Rev. Lett. **59**, 1691 (1987).

[18] R. J. Phaneuf and E. D. Williams, Surf. Sci. **195**, 330 (1988). Note that this work also reports step measurements that suggest that the details of the equilibrium shape near (111) differ from that reported here.

[19] Y-N. Yang and E. D. Williams, J. Vac. Sci. Technol. A **8**, 2481 (1990).

[20] D. J. Eaglesham, G. S. Higashi, and M. Cerullo, Appl. Phys. Lett. **59**, 685 (1991).

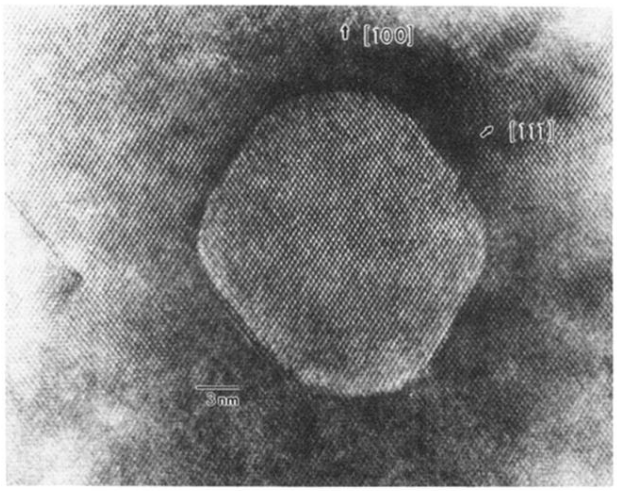

FIG. 1. The equilibrium shape of Si. Typical annealed void shape imaged in high resolution down ⟨110⟩ axis. Void is small enough to be completely enclosed in transmission electron microscopy cross section. Note flat {111} facets and rounded {100} facets, and curved facet intersections at {100} and near {311}.